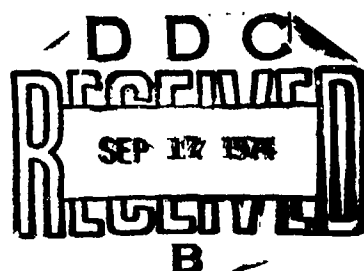


UNCLASSIFIED

AD NUMBER
AD922294
NEW LIMITATION CHANGE
TO Approved for public release, distribution unlimited
FROM Distribution limited to U.S. Gov't. agencies and their Contractors; Specific authority; 11 Sep 74. Other requests must be referred to Director, Defense Advanced Research Projects Agency, Attn: TIO. Arlington, Va. 22209.
AUTHORITY
ONR ltr dtd 7 Oct 1998

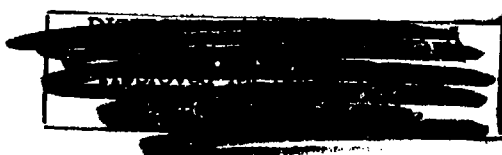
THIS PAGE IS UNCLASSIFIED

✓
1
AD 922294



NORTHROP

Research and Technology Center



✓
Distribution limited to U.S. Gov't. agencies only!
Test and Evaluation: 11 SEP 1974. Other requests
for this document must be referred to

ARPA - TIO ARL VA 22209

NRTC 74-33R

HIGH POWER CO LASER
QUARTERLY TECHNICAL REPORT

Period Covering:
March 1, 1974 - May 31, 1974

July 1974

Prepared by

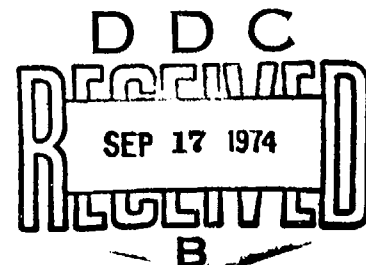
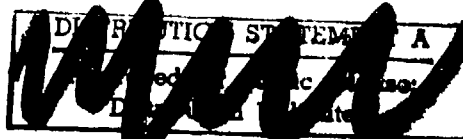
Northrop Research and Technology Center
G. L. McAllister, D. K. Rice, V. G. Draggoo

Contract N00014-72-C-0043

Sponsored by
ADVANCED RESEARCH PROJECTS AGENCY
ARPA ORDER NO. 1807

Monitored by
OFFICE OF NAVAL RESEARCH
CODE 421

NORTHROP CORPORATION
Northrop Research and Technology Center
Laser Technology Laboratories
3401 West Broadway
Hawthorne, California 90250



UNCLASSIFIED

SECURITY CLASSIFICATION OF THIS PAGE (When Data Entered)

REPORT DOCUMENTATION PAGE		READ INSTRUCTIONS BEFORE COMPLETING FORM
1. REPORT NUMBER NRTC 74-33R	2. GOVT ACCESSION NO.	3. RECIPIENT'S CATALOG NUMBER
4. TITLE (and Subtitle) High Power CO Laser Quarterly Technical Report - Period Covering: March 1, 1974 - May 31, 1974		5. TYPE OF REPORT & PERIOD COVERED Quarterly Technical Report
7. AUTHOR(s) G. L. McAllister, D. K. Rice, V. G. Draggoo		6. PERFORMING ORG. REPORT NUMBER
9. PERFORMING ORGANIZATION NAME AND ADDRESS Northrop Research and Technology Center 3401 West Broadway Hawthorne, California 90250		8. CONTRACT OR GRANT NUMBER(s) N00014-72-C-0043
11. CONTROLLING OFFICE NAME AND ADDRESS Advanced Research Projects Agency 1400 Wilson Blvd. Arlington, Virginia		10. PROGRAM ELEMENT, PROJECT, TASK AREA & WORK UNIT NUMBERS ARPA Order No. 1806
14. MONITORING AGENCY NAME & ADDRESS (if different from Controlling Office) Office of Naval Research Department of the Navy Arlington, Virginia 22217		12. REPORT DATE July 1974
		13. NUMBER OF PAGES
		15. SECURITY CLASS. (of this report) Unclassified
		15a. DECLASSIFICATION/DOWNGRADING SCHEDULE
16. DISTRIBUTION STATEMENT (of this Report)		
17. DISTRIBUTION STATEMENT (of the abstract entered in Block 20, if different from Report)		
18. SUPPLEMENTARY NOTES		
19. KEY WORDS (Continue on reverse side if necessary and identify by block number)		
CO Laser Molecular Kinetics Energy/Power Molecular Lasers Unstable Resonators Measurements Electrical Discharge Lasers Mode Theory Line Selection High Power Lasers High Efficiency		
20. ABSTRACT (Continue on reverse side if necessary and identify by block number)		
<p>Effort on the High Power CO Laser Program is reviewed. The program is directed toward the development of the required CO laser technology, the required component technology, and the design and construction of intermediate power laser devices. The results of analytical and experimental investigation of the basic characteristics of the laser and data from a high pressure electrically excited CO laser device are discussed.</p>		

DD FORM 1473 EDITION OF 1 NOV 65 IS OBSOLETE

ii

UNCLASSIFIED

SECURITY CLASSIFICATION OF THIS PAGE (When Data Entered)

PROGRAM IDENTIFICATION

ARPA Order No. : 1807

Program Code No. : 3E90

Name of Contractor: Northrop Corporation

Effective Date of Contract: 30 September 1974

Amount of Contract: \$3,650,663

Contract No. : N00014-72-C-0043

Program Manager: Dr. G. L. McAllister
(213) 675-4611, Ext. 4975

Scientific Officer: Director, Physics Program
Physical Sciences Division
Office of Naval Research
Department of the Navy
800 North Quincy
Arlington, Virginia 22217

Disclaimer: The views and conclusions contained in this document are those of the authors and should not be interpreted as necessarily representing the official policies, either expressed or implied, of the Advanced Research Projects Agency or the U. S. Government.

TABLE OF CONTENTS

1.0	INTRODUCTION	1
2.0	SPECTRAL LINE SELECTION	2
3.0	BEAM DIAGNOSTIC MEASUREMENTS WITH THE 10-LITER LASER	9
3.1	Beam Diagnostic Configurations	9
3.2	Beam Diagnostic Measurements	9
3.3	Effects of Acoustical Disturbances	18
3.4	Conclusions from Beam Diagnostic Experiments	21
	REFERENCES	22

TABLE OF CONTENTS

1.0	INTRODUCTION	1
2.0	SPECTRAL LINE SELECTION	2
3.0	BEAM DIAGNOSTIC MEASUREMENTS WITH THE 10-LITER LASER	9
3.1	Beam Diagnostic Configurations	9
3.2	Beam Diagnostic Measurements	9
3.3	Effects of Acoustical Disturbances	18
3.4	Conclusions from Beam Diagnostic Experiments	21
	REFERENCES	22

1.0 INTRODUCTION

During this reporting period, detailed measurements of the laser beam quality were made and preliminary line selection data was obtained. It was found that greater than 80% of the theoretical energy is contained in the central lobe of the far-field intensity pattern excluding approximately 25% of the beam which is refracted out due to density disturbances resulting from bulk heating of the laser medium. Spectral measurements were made for CO/Ar and CO/N₂ gas mixtures with the intracavity water vapor cell and, although it proves to be effective for rotational line selection, the electrical excitation rate was not sufficient to obtain the lower vibrational bands and the efficiency was consequently low.

The intracavity water vapor absorption cell was operated with water vapor pressures from 0 Torr to 1000 Torr. As the water vapor content was increased, the spectral emission shifted gradually to the best rotational line in each vibrational band. In addition the loss was sufficient to inhibit the vibrational transitions higher than 7 → 6. The electrical excitation rates used were low and the only strong band having high atmospheric transmittance was the 6 → 5 band. Four hundred (400) Torr of water vapor in the absorption cell was sufficient to shift most of the 6 → 5 output to P₉ which is the best line. With this amount of water vapor the efficiency had degraded only 35% even though the higher bands were highly attenuated.

The beam diagnostic measurements were made by imaging the far-field intensity profile (at the focal plane of a lens) onto an integrating pyro-electric detector array. Both one-dimensional and two-dimensional measurements have been made and the results agree closely with the theoretical predictions. The major degradation is produced by the density disturbances which cause vertical stripes to be superimposed on the far-field pattern. These density disturbances are shown to be due to bulk heating of the laser medium and both their magnitude and their effect are described.

2.0 SPECTRAL LINE SELECTION

During this reporting period the large aperture intracavity water vapor absorption cell system was integrated into the nominal 10-liter CO EDL system. The details of the cell system have been described previously.¹ The initial line selection experiments were conducted with the stable resonator configuration illustrated in Figure 2.1. The output coupler is a 13.0 cm diameter flat calcium fluoride substrate with an antireflection coating on one surface and a 28% reflective coating on the other side. The rear reflector is an 11.8m radius beryllium copper substrate with a silver enhancement and dielectric protective coating. The cavity length is 4.4m. The clear aperture of the system is approximately 9cm.

The purpose of these initial experiments was to confirm the results of previous investigations²⁻⁹ by verifying the feasibility of the spectral line selection of a CO EDL and to obtain the approximate operating parameters of the water vapor absorption cell. The diagnostic setup for these experimental investigations are shown in Figure 2.2. The spectral information was recorded photographically from the fluorescent screen of the spectrometer (Optical Engineering CO Spectrum Analyzer). Output energy was measured using the reflected energy from a 2.7% reflecting calcium fluoride beam splitter (antireflection coating on one side) and a calorimeter (Hadron Series 117 Ballistic Thermopile). The temporal shape of the output pulse was monitored with a Au:Ge detector (Cryogenics Associates).

Typical data are illustrated in Figure 2.3. The spectral output with the water vapor cell evacuated is shown in Figure 2.3a for the laser operating parameters listed. For the low electrical input pumping rate the spectra consists of lines corresponding to transitions in the vibrational bands 5-4 to 11-10. Kinetic modeling investigations predict that as the level of electrical pumping is increased relative to V-V pumping, the output spectra shifts toward the lower vibrational bands.¹⁰⁻¹¹ It is the low vibrational bands (6-5 and below) which

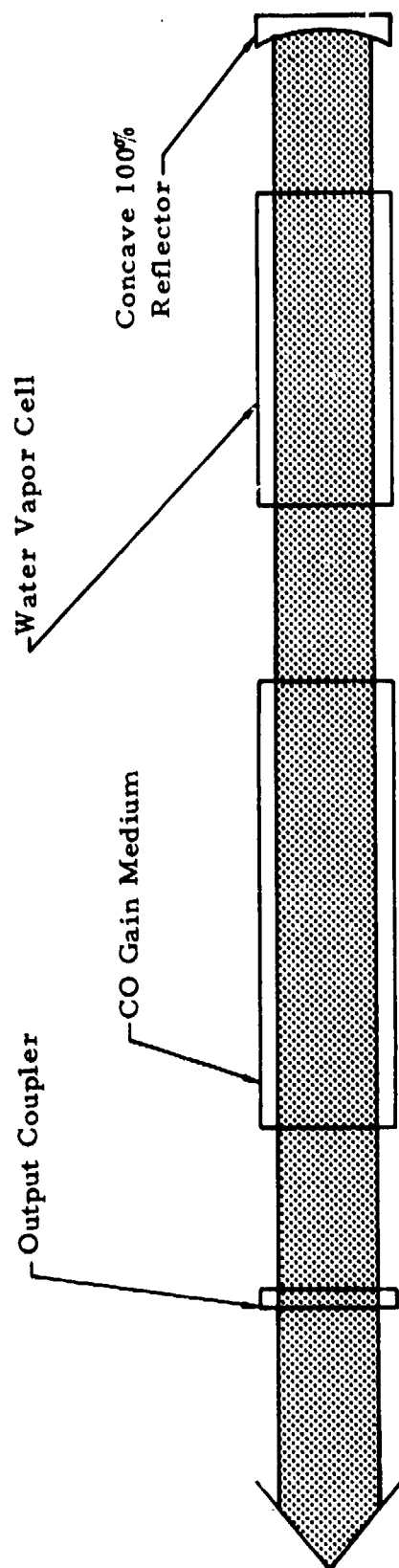


Figure 2.1. Spectral line selection configuration for nominal 10 liter CO EDL with stable resonator optics.

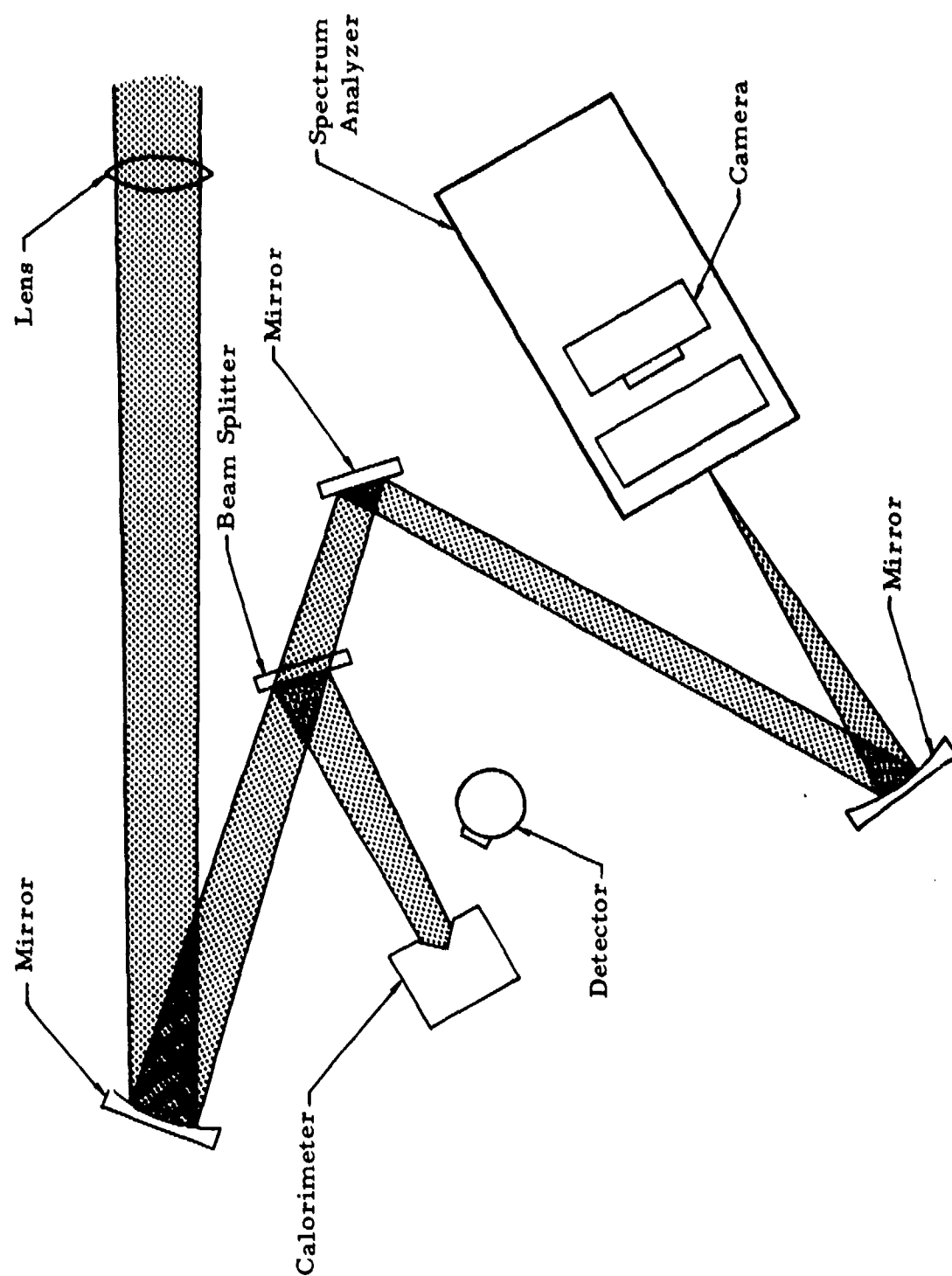
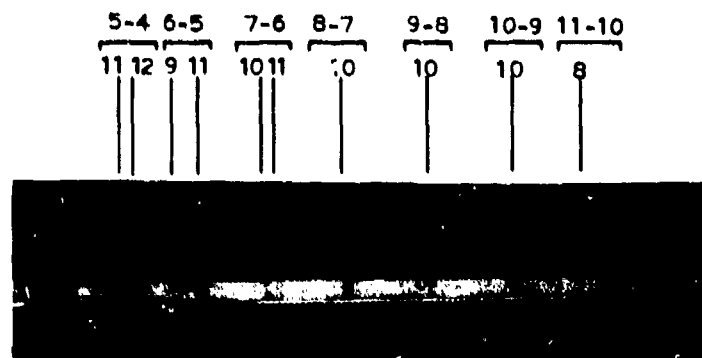
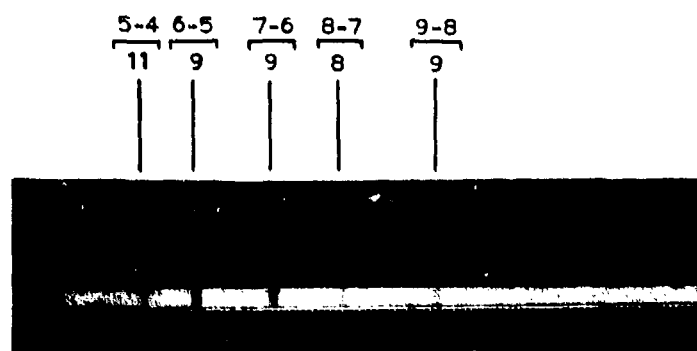


Figure 2.2. Diagnostic configuration for spectral line selection of nominal 10 liter CO EDL.



a. $P(\text{H}_2\text{O}) \approx 0$ Torr



b. $P(\text{H}_2\text{O}) \approx 600$ Torr @ 155°C

$$P_T = 85 \text{ Torr}$$

$$\text{N}_2:\text{CO} = 10:1$$

$$W_{\text{IN}} = 850 \text{ W/cm}^3 (\Delta T \approx 80 \mu\text{sec})$$

$$T = 80^\circ\text{K}$$

Figure 2.3. Output spectra of nominal 10 liter CO EDL with and without line selection.

have the highest predicted atmospheric transmission. However, for the purposes of these preliminary experiments, no attempt was made to achieve the pumping required to limit oscillation to these low V-bands. Figure 2.3b shows the effect of 600 Torr of water vapor at a temperature of 155°C in the absorption cell on the output spectra. Note that lines in the 11-10 and 10-9 bands have been eliminated and the lines in the other bands have shifted.

Figure 2.4 shows the effect of various amounts of water vapor in the absorption cell on the spectral performance of the laser for the operating parameters listed. This is an extension of the data of Figure 2.3. The value listed above each spectral line is the predicted atmospheric attenuation e-folding distance for the Midlatitude Winter Atmospheric Model at sea level.⁴ The height of each line is a qualitative representation of its relative intensity as interpreted from the photographic data such as illustrated in Figure 2.3. As the water vapor content is increased, the laser oscillation within a particular vibrational band tends to shift to those lines having highest atmospheric transmittance. For example, with no water vapor the 6-5 band has two rotational lines present, P(9) and P(11), which have predicted e-folding distances of 13.51km and 1.75km respectively. The P(9) is barely detectable and the P(11) is the most intense line in the spectra. As the amount of water vapor in the cell is increased, the relative intensities of the two lines reverse and when 600 Torr of water vapor is present only the P(9) line oscillates. In addition to the rotational line selection a certain amount of vibrational line selection has occurred as evidenced by elimination of the 11-10, 10-9, and 9-8 transitions when 1000 Torr of water vapor is present. The gain for the 5-4 band is such that that even the low loss introduced for the high transmittance lines of this band is too much to sustain oscillation on these lines.

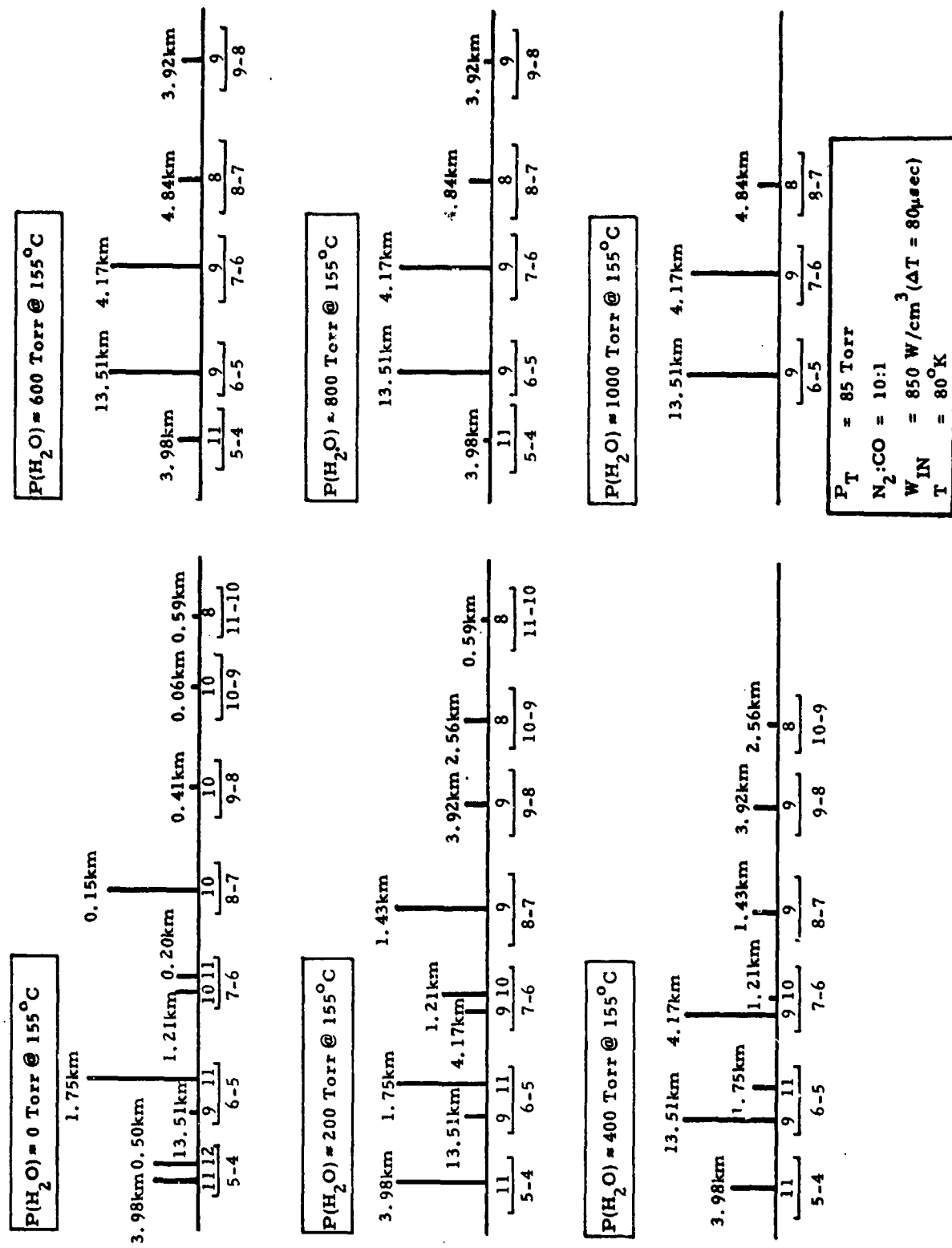


Figure 2.4. Output spectra of nominal 10 liter CO EDL as a function of water vapor content of absorption cell.

Since the output spectra included lines in the vibrational bands 7-6 and above, the addition of water vapor to the absorption cell was anticipated to have a substantial effect on the efficiency of the laser as a result of vibrational line selection. The output energy without line selection was 114J. With 200 Torr of water vapor the output was 89J; 400 Torr - 71J; 600 Torr - 56J; 800 Torr - 45J; 1000 Torr - 29J. Thus the loss of efficiency appears primarily attributable to the effect of the water vapor on the upper V-bands. During the next reporting period the electrical input will be adjusted to provide for the pumping necessary to obtain laser action on the 6-5 bands and below. Full aperture stable resonator experiments will be performed with this electrical pumping. Following these investigations the compound unstable resonator configuration will be utilized in conjunction with the line selection experiments.

3.0 BEAM DIAGNOSTIC MEASUREMENTS WITH THE 10-LITER LASER

During this reporting period, detailed measurements of the 10-liter laser beam quality were made using an integrating pyroelectric detector array. The central lobe of the far-field pattern contained greater than 80% of the theoretical energy excluding approximately 25% of the beam which is refracted out due to the acoustical waves generated by bulk heating of the medium. The measurement techniques and results are described in the sections below.

3.1 Beam Diagnostic Configurations. The diagnostic configuration used for measuring the laser beam quality is illustrated in Figure 3.1. The laser output was focused with a 5.5m focal length CaF_2 lens and the output reduced in intensity using CaF_2 beam splitters. The image at the focal plane was magnified approximately a factor of 10 and imaged onto an integrating linear pyroelectric detector array (Laser Precision Model AK2930/64). This array has 64 1mm x 1mm elements separated by 0.1mm and thus produces, for each shot, an intensity profile across the focal plane with approximately 0.1mm resolution. Single shot profiles were taken through the beam center in both the horizontal and vertical directions and compared with theory. A two-dimensional profile of the focal plane image was generated by successively translating the magnifying lens a small distance (typically <0.1mm) vertically between each shot.

3.2 Beam Diagnostic Measurements. The e^- -beam stabilized 10-liter CO EDL has been described in previous reports.¹⁻² Measurements of the beam profiles were made for CO/Ar and CO/ N_2 gas mixtures for energies up to 350J. The observed far-field pattern(at the focal plane) is a series of concentric rings similar to an Airy pattern with a superimposed vertical stripe. This stripe is caused by energy refracted from the beam by the density variations in the laser medium produced by the medium heating.

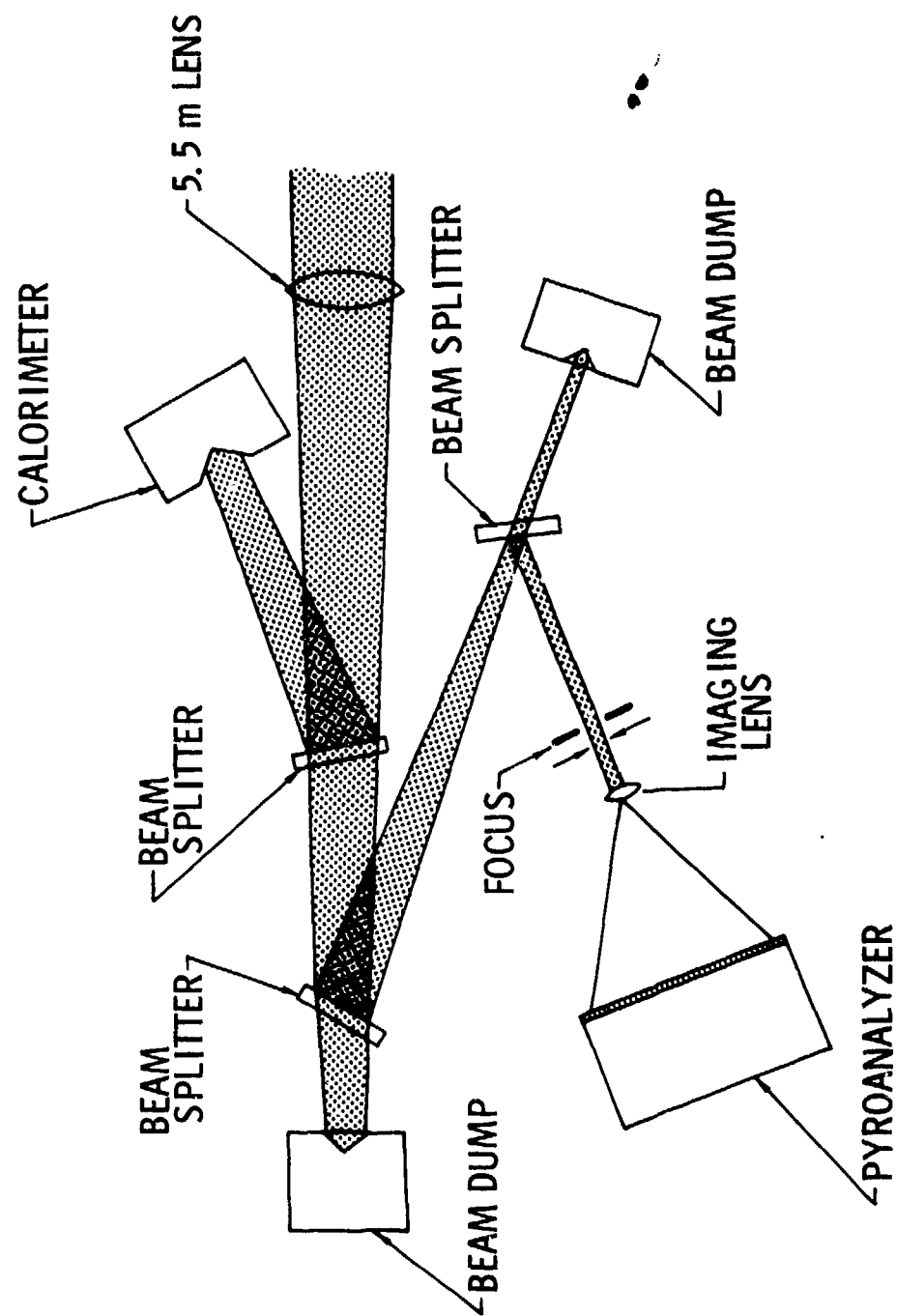


Figure 3.1. Diagnostic configuration used for beam intensity profile measurements.

An example of this pattern is shown by the plexiglas burn records illustrated in Figure 3.2. The vertical stripe accounts for approximately 25% of the energy for CO/N₂ gas mixtures and is discussed in Section 3.3. A discussion of the measurements of the central part of the beam follows below.

A confocal unstable resonator was used with a truncated circular mask defining the outer radius. This mask, illustrated in Figure 3.3, is truncated so that vignetting does not occur at the laser discharge boundaries. The output was thus approximately an annulus with 2:1 ratio for the outer and inner radii, and it is this annulus (uniformly illuminated) to which the experimental results are compared. The beam was focused with the 5.5m focal length CaF₂ lens and compared with the theoretical pattern predicted for the uniformly illuminated annulus. A typical pyroanalyzer trace giving a horizontal intensity profile through the beam center is compared with the theoretical trace in Figure 3.4. The agreement is excellent except for the slight increase in the first side lobe on the left side.

A smooth curve was drawn through the pyroanalyzer data in Figure 3.4. The two sides were averaged and the result integrated to determine the energy contained within a circle of arbitrary radius. The result of this integration is compared to the theoretical value in Figure 3.5. Approximately 80% of the theoretical energy is contained in the central lobe and this value increases with radius.

More detailed measurements were made for a CO/N₂ (1:5) gas mixture at 100 Torr and 80°K. A series of horizontal profiles were taken for energies at approximately 100J with the vertical position stepped with each shot so that the entire beam profile could be measured. These profiles were normalized to the laser output energy and were then entered into the CDC 6600 computer. Subroutine DISPPLA was used to give three-dimensional projections of the focal plane intensity profile. Figures 3.6 and 3.7 show two projections of this profile. It should be emphasized that not only does the

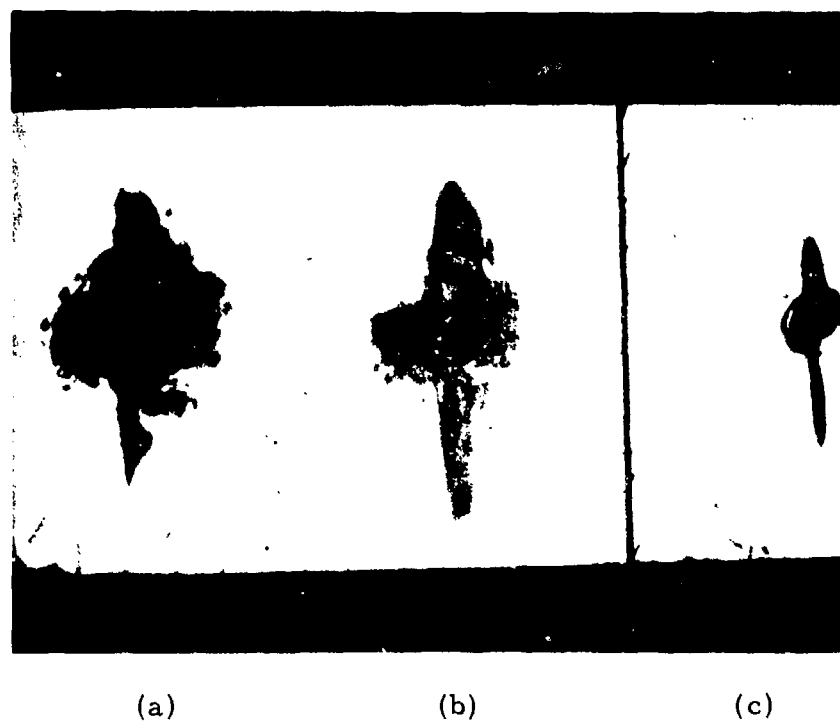


Figure 3.2. Plexiglas burn patterns for (a) a CO/Ar gas mixture (100J), (b) a CO/N₂ gas mixture (100J) and (c) a CO/N₂ gas mixture (50J).

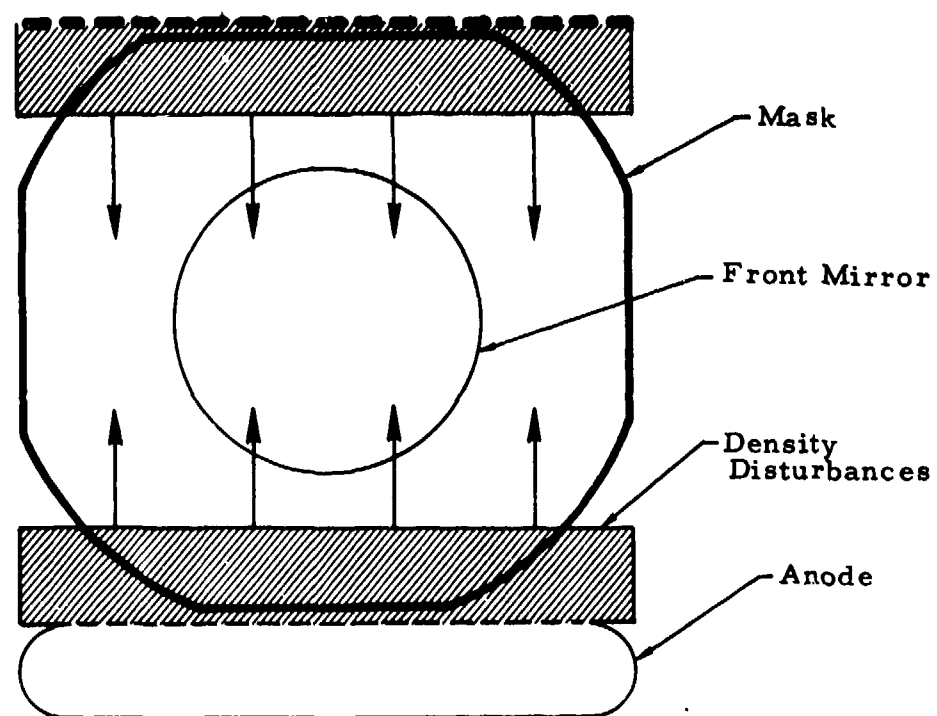


Figure 3.3. Laser cavity configuration illustrating the density disturbances and the aperturing mask.

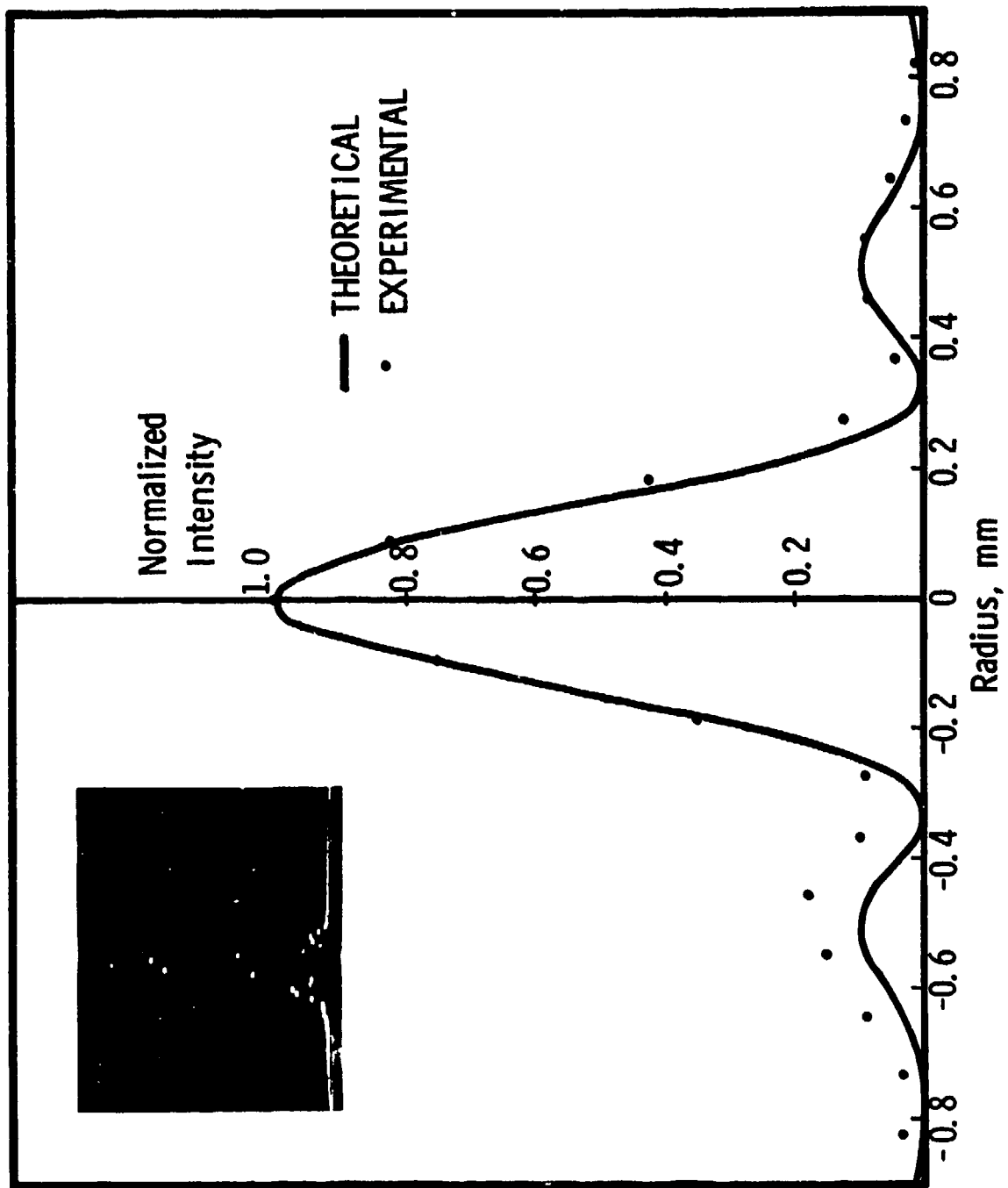


Figure 3.4. Pyroanalyzer trace of laser intensity profile at the focus compared with the theoretical profile.

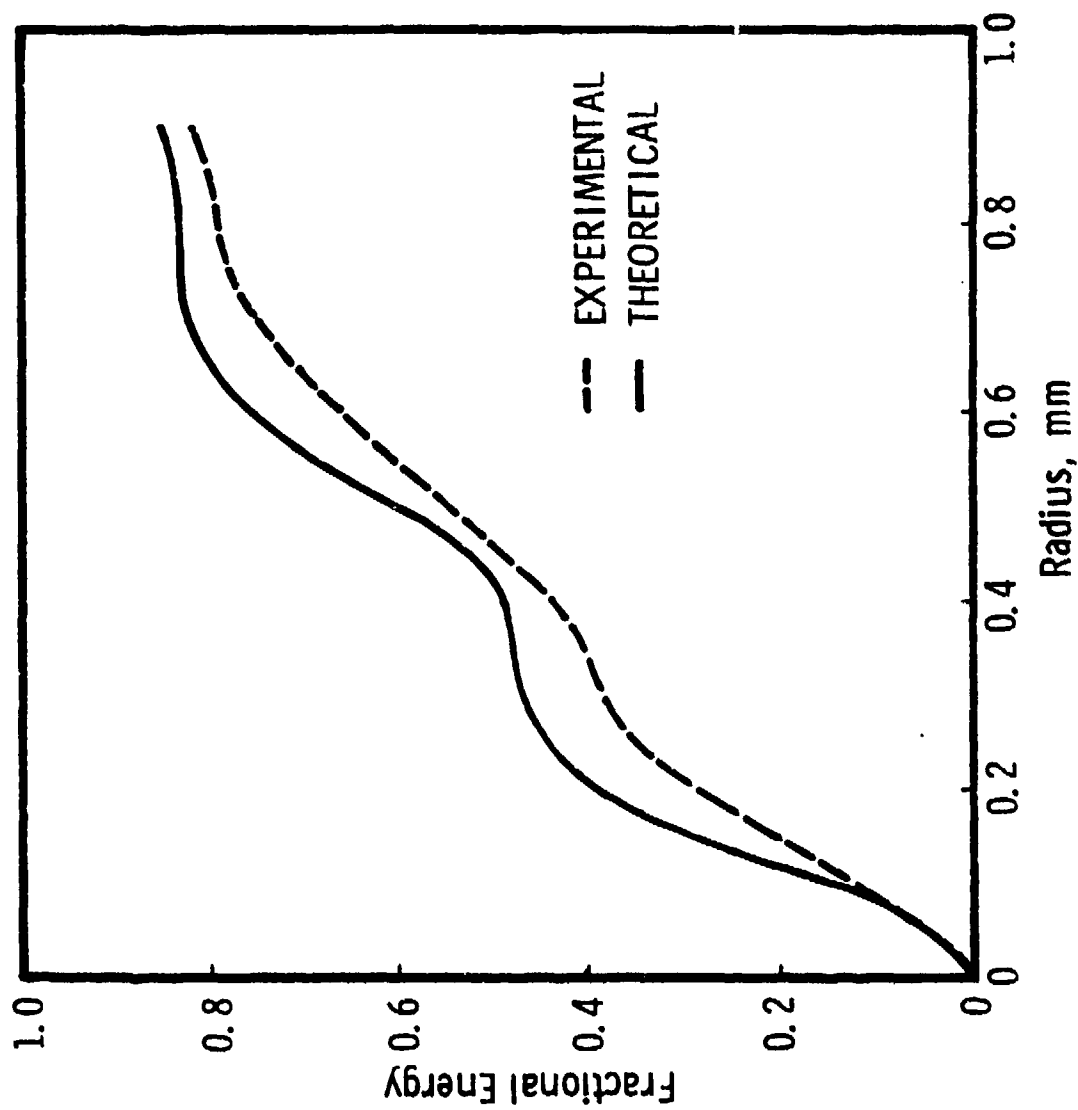


Figure 3.5. Comparison of the experimental and theoretical energies contained within an arbitrary radius at the focal plane.

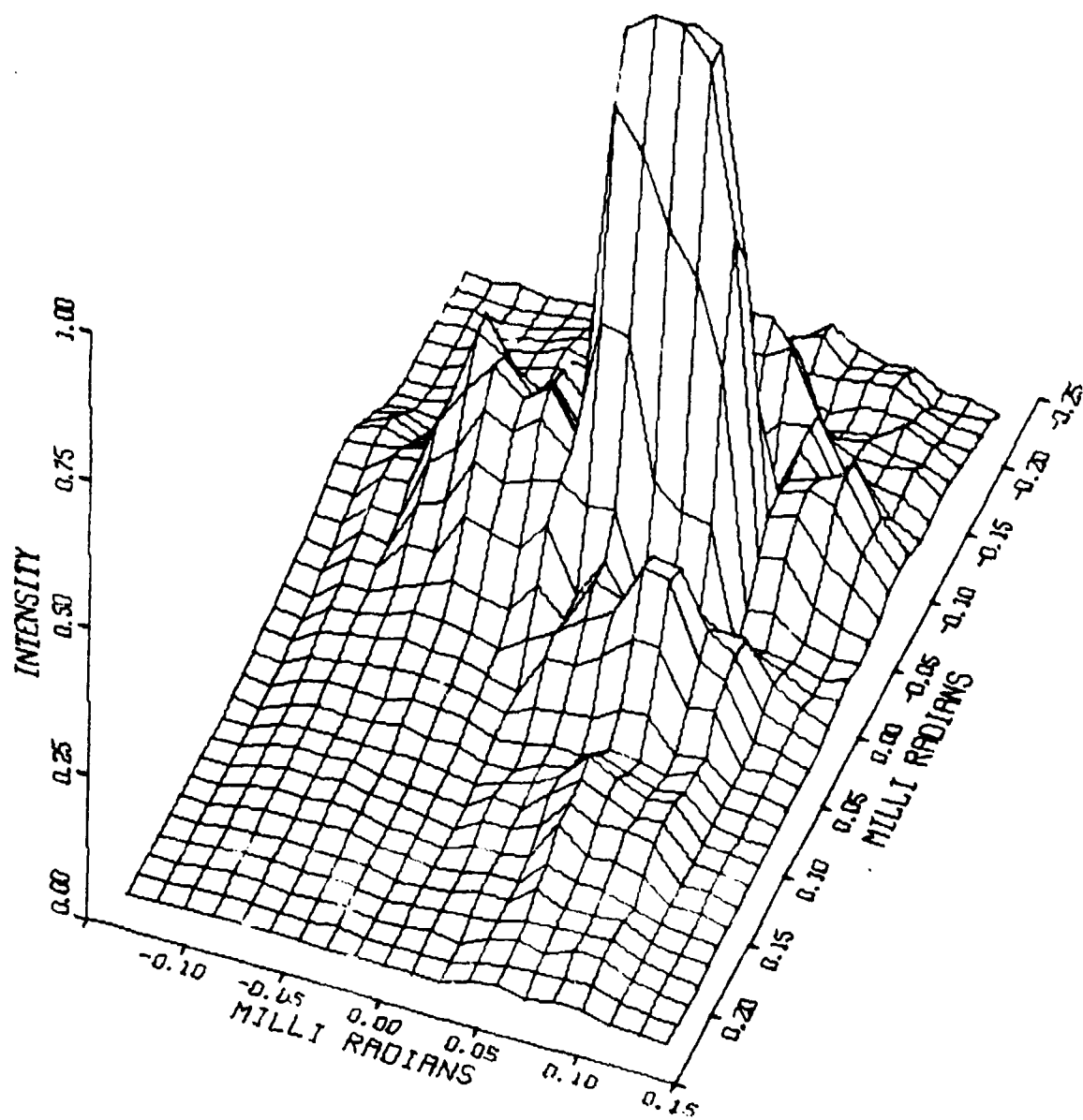


Figure 3.6. Two-dimensional experimental profile of the laser intensity in the focal plane of a 5.5m lens.

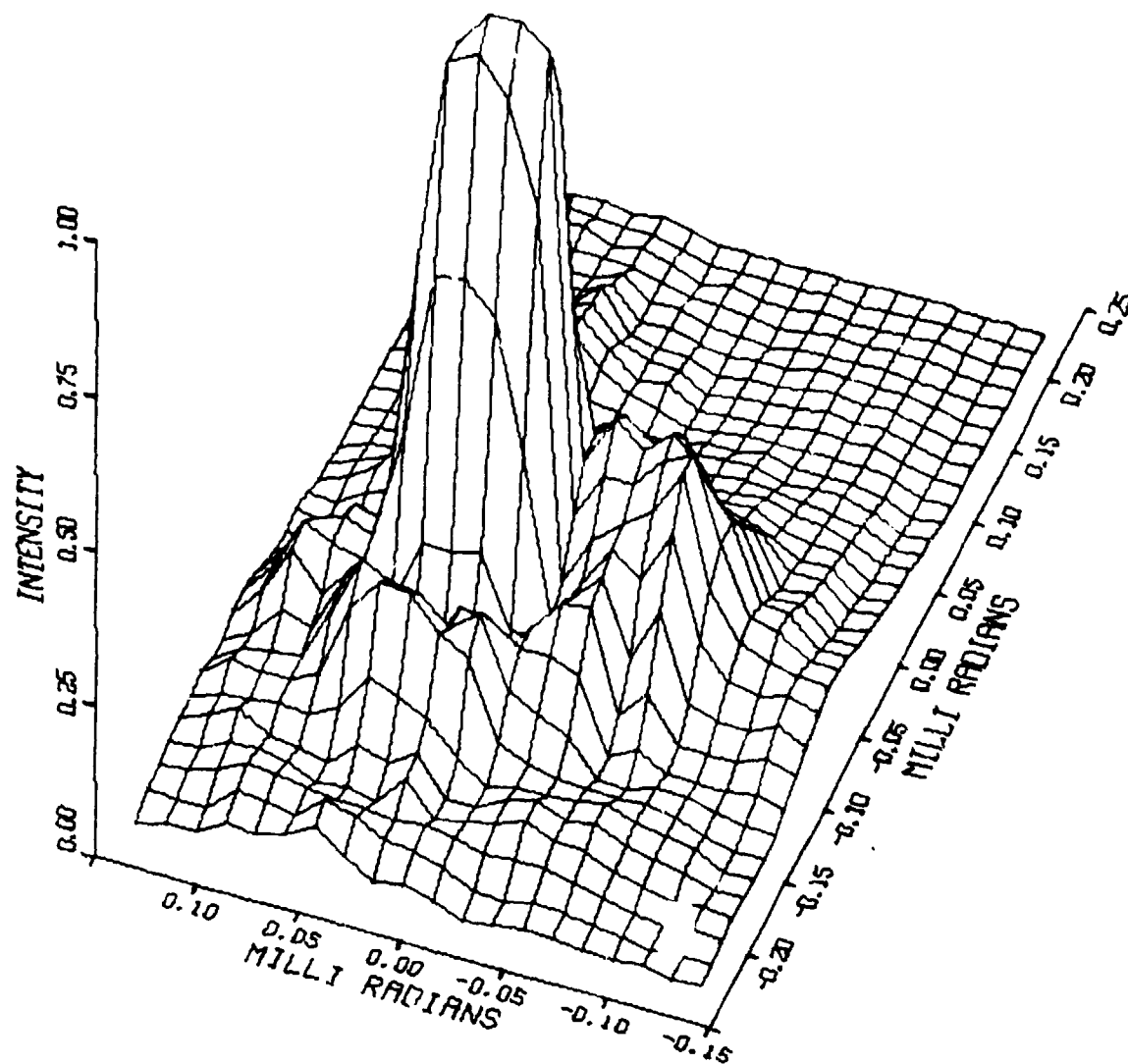


Figure 3.7. Two-dimensional experimental profile of the laser intensity in the focal plane of a 5.5m lens.

single shot data compare well with the theory but the shot-to-shot repeatability corresponds to an angular accuracy (over 20 or more shots) better than $20\mu\text{rad}$.

3.3 Effects of Acoustical Disturbances. The 10-liter device is constructed¹⁻² such that the cathode is very porous, the anode is slightly porous and the Lexan sidewalls are solid. Bulk heating of the laser gas thus creates a pressure gradient which forces laser gas out of the cavity with resulting rarefaction waves which enter the medium from both the cathode (top) and the anode (bottom). In addition the intense heating in the cathode fall region generates a step function in the density during the time that the electrical excitation is on which also propagates into the medium. These disturbances have been studied with a Mach-Zehnder interferometer in order to determine the bulk heating rate. The experimental configuration and typical results were described in the previous report.¹ The analysis of these data is nearly completed and it is found¹² that the heating rate depends weakly on the electrical excitation conditions and the gas mixtures used but is typically less than 15%. A typical density profile and the corresponding Mach-Zehnder interferogram are shown in Figure 3.8. The density disturbances propagate toward the horizontal center line of the cavity at the acoustical velocity and act as prisms² which refract that part of the beam which passes through these regions. It is evident from the interferogram in Figure 3.8 that the density disturbances³ act approximately like linear prisms. Optical radiation emitted near the cathode is refracted downward and radiation emitted in the vicinity of the anode is refracted upward. The resultant angle of refraction depends on the laser gas refractive index, the electrical excitation rate and the bulk heating rate, i.e. the rate at which electrical energy is converted to thermal energy. The anode is only slightly porous thus the density variation (and the resultant angle of refraction) is smaller than the corresponding variation at the cathode. Typical values for angles of refraction are $\Theta_{\text{cathode}} = 700 \mu\text{rad}$ and $\Theta_{\text{anode}} = 350 \mu\text{rad}$. The refracted beams are thus displaced by 4mm and 2mm in the focal plane of the 5.5m CaF_2 lens.

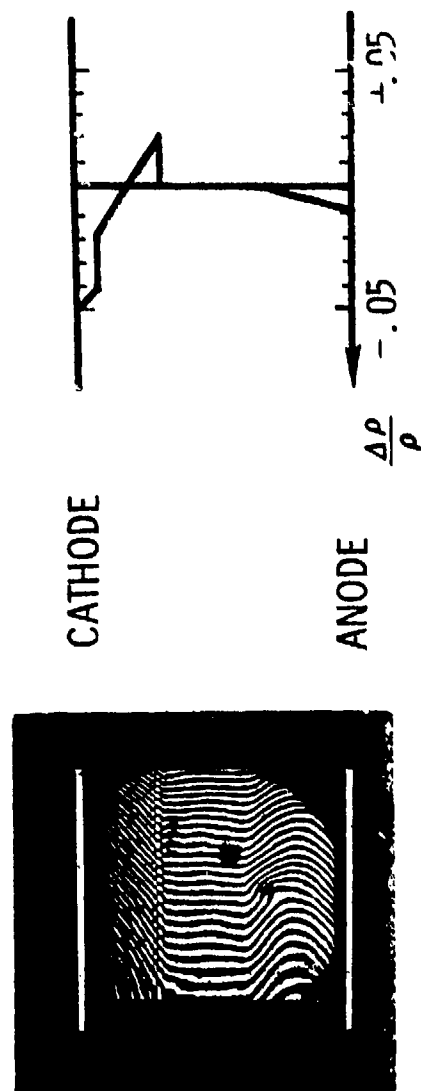


Figure 3.8. Mach-Zehnder interferometer measurements showing the density perturbations for the CO EDL.

Initially only a small thickness of the beam is affected and diffraction causes the refracted beams to also be spread over several millimeters in the vertical direction at the focal plane. As time progresses and the density wave moves into the cavity the affected region becomes larger so the total energy refracted out of the beam becomes greater. At the same time the vertical spreading due to diffraction becomes less. This is illustrated by the shaded areas in Figure 3.3 which represent the region affected by the density waves moving toward the cavity center. By the time laser emission occurs the wave has progressed to the point where the widths of the refracted beams are at least half the aperture diameter and diffractive spreading in the horizontal direction is thus not very significant. The net result is, as stated previously, a central pattern (produced by the undisturbed medium) resembling an Airy pattern and a vertical stripe (produced by the disturbed medium) superimposed upon it.

The energy contained in this vertical stripe was measured and computed to be approximately 25% of the total beam energy. The peak intensity in the stripe is approximately 5% that of the central spot peak intensity and the area approximately 15 times the central lobe (excluding the stripe). This leaves 25% of the total beam in the stripe. This number was verified by taking a typical temporal intensity profile and computing what fraction of the total beam (assuming uniform illumination) is affected at each point in time. This approach is in agreement with the experimental measurements in that again approximately 25% is refracted into the stripe. Additional verification of these results was obtained by looking only at the stripe with a Ge: Au detector. When the near-field pattern is masked near the cathode, there is a delay in the appearance of the detected intensity which corresponds to the acoustical transit time from the cathode to the bottom of the mask.

3.4 Conclusions from Beam Diagnostic Experiments. Characteristically, CO/N₂ gas mixtures result in laser pulses which last for several tens of microseconds after the electrical excitation is turned off as energy stored in the nitrogen vibrational levels is transferred back to CO. Thus it would at first seem that dilute mixes (high N₂ content), which give better laser performance, would be undesirable because more of the pulse would be refracted out of the main beam. This dependence is very weak, however, because the dilute mixtures also reach threshold earlier and the effects nearly cancel.

Argon/CO mixtures also produce a pulse with a tail on it but it is considerably shorter since argon does not store energy. As expected, the fractional percentage into the vertical stripe is less. This is evident from Figure 3.2 which shows both CO/N₂ and CO/Ar burn patterns at approximately the same energy.

It is concluded that the beam quality of the device is excellent and that the major degradation is caused by the density waves generated by bulk heating. If necessary, these effects can be minimized by using argon as a diluent and/or by pumping harder for shorter pulse durations. In general as the excitation time is decreased the allowable E/N (without arcing) can be increased. Thus the pulse lengths can be shortened somewhat without proportionally reducing the energy out.

REFERENCES

1. G. L. McAllister, W. B. Lacina, D. K. Rice and P. J. Mendoza, "High Power CO Laser Semiannual Technical Report," (May 1974).
2. Northrop Report NLSD 72-7R, "Semi Annual Technical Status Report, High Power CO Laser," March 1972.
3. D. K. Rice, "Absorption Measurements of Carbon Monoxide Laser Radiation by Water Vapor," AD 746-170 (July 1972).
4. D. K. Rice, "Carbon Monoxide Spectral Line Selection Studies," AD 749-823 (August 1972).
5. Northrop Report NRTC 72-10R, Fourth Quarterly Technical Status Report, High Power CO Laser, " September 1972.
6. D. K. Rice, "Absorption Measurements of Carbon Monoxide Laser Radiation by Water Vapor," presented at Autumn Meeting of Optical Society Association, 17-20 October 1972, San Francisco, California.
7. D. K. Rice, "Absorption Measurements of Carbon Monoxide Laser Radiation by Water Vapor," Appl. Opt., Vol. 12, No. 2, pp 218-225 (February 1973).
8. D. K. Rice, G. L. McAllister, R. G. Eguchi, and M. M. Mann, "High Efficiency Operation and Spectral Line Selection of a High Pressure CO Laser," Paper 11-A presented at 1973 IEEE/OSA Conference on Laser Engineering and Applications (Washington, D.C.), 30 May - 1 June 1973.
9. Northrop Report NRTC 73-38R, "Sixth Quarterly and Semiannual Report, High Power CO Laser," November 1973.
10. W. B. Lacina and M. M. Mann, "Transient Oscillator Analysis of a High Pressure Electrically Excited CO Laser," Appl. Phys. Lett., 21, 224 (1972).
11. W. B. Lacina, M. M. Mann, and G. L. McAllister, "Transient Oscillator Analysis of a High Pressure Electrically Excited CO Laser," IEEE, J. Quant. Electron., QE-9, 588 (1973).
12. F. E. C. Culick, P. I. Shen, W. S. Griffin, "Studies of Acoustic Waves Formed in an Electric Discharge CO Laser Cavity," to be published.



DEPARTMENT OF THE NAVY
OFFICE OF NAVAL RESEARCH
800 NORTH QUINCY STREET
ARLINGTON, VA 22217-5660

IN REPLY REFER TO

5510/6
Ser 93/886
7 Oct 98

From: Chief of Naval Research
To: Administrator
Defense Technical Information Center
ATTN: William Bush, DTIC-OCQ
8725 John J. Kingman Road Suite 0944
Ft. Belvoir, VA 22060-6218

Subj: CHANGE OF DISTRIBUTION STATEMENT

1. Permission is granted to change the distribution statement for the following documents to Distribution Statement A: Approved for Public Release; Distribution is Unlimited:

AD 525 354

AD 529 106

AD 922 294

2. Questions may be directed to the undersigned on (703) 696-4619.

A handwritten signature in cursive script, reading "Peggy Lambert", is written over a horizontal line.

PEGGY LAMBERT
By direction